Contribution to a Harmonized Test Methodology to Compare Railway Wireless Communication Technologies Under Transient Interference

Artur Nogueira de São José, Nathan Chopinet, Eric Pierre Simon, Virginie Deniau, Norbert Becuwe

Contribution to a harmonized test methodology to compare railway wireless communication technologies under transient interference

Artur N. de São José, Nathan Chopinet, Eric Pierre Simon, Virginie Deniau, and Norbert Becuwe

***Abstract*—A growing number of wireless communication systems are being installed on trains to improve safety and passenger comfort. However, most communication antennas are located on the roof of the train, close to the aerial supply lines and the pantograph-catenary interface. Due to the recurrent loss of contact at this interface, a high difference of potential inevitably generates frequent electric arcs, resulting in transient radiated electromagnetic disturbances sensed by the communication antennas. In a context where the railway industry is looking for new wireless technologies to replace the existing ones, an essential criterion for choosing one technology over the other is the resistance to the transients generated by the pantograph-catenary contact. In this paper, we propose a test methodology that fills a gap in the electromagnetic compatibility literature since the immunity test standards are mainly dedicated to product validation and not to the evaluation of communication systems. Our methodology has been evaluated through experiments based on a common resilience metric that allows comparison between two different communication systems used in railways: LTE and LoRaWAN.**

***Index Terms*—Wireless systems EMC, Radiated immunity and emissions, Internet of things (IOT), Railway systems.**

I. Introduction

MODERN trains are equipped with wireless communication systems which traditionally perform tasks such as voice communication, signaling, and command-control. The global system for mobile communications-railway (GSM-R) technology is the harmonized standard in Europe for voice and data communication used by the railway staff. However, other market demands like the internet on board, remote maintenance, and remote train control have technical requirements that GSM-R cannot fulfill. To accomplish these tasks, emerging technologies based on the internet-of-things (IoT) [1], augmented reality [2], etc., dispute the railway market.

This work was performed in the framework of the LoRa-R project, which is co-financed by the European Union with the European Regional Development Fund, the Hauts-de-France Region Council, and the SNCF railway company.

Artur N. de São José, Nathan Chopinet and Virginie Deniau are with COSYS-LEOST, Univ Gustave Eiffel, IFSTTAR, Univ Lille, 59650 Villeneuve d'Ascq, France (e-mail: artur.nosj@gmail.com; nathan.chopinet@univ-eiffel.fr; virginie.deniau@univ-eiffel.fr).

Eric Pierre Simon is with Univ. Lille, CNRS, USR 3380 - IRCICA - Institut de Recherche sur les Composants logiciels et matériels pour l'Information et la Communication Avancée, F-59000 Lille, France and also with Univ. Lille, CNRS, Centrale Lille, Univ. Polytechnique Hauts-de-France, UMR 8520 - IEMN, F-59000 Lille, France (e-mail: eric.simon@univ-lille.fr).

Norbert Becuwe is with the National French Railway company-SNCF-Ingénierie du Matériel, F-59260 HELLEMMES, France (e-mail: norbert.becuwe@sncf.fr).

In this context, there is competition not only between companies that provide wireless solutions for specific applications (*e.g.* Semtech and SigFox in the IoT market) but also between general-purpose technologies such as long-term evolution (LTE) [3] and 5G [4], [5]. In particular, 5G has the potential to adaptively provide network resources to applications with different requirements. In this way, the railway industry employs and introduces new communication technologies on board trains in addition to GSM-R to ensure complementary services. Figure 1 summarizes this situation.

In the scenario illustrated in Fig. 1, certain questions may arise, such as:

- which IoT technology can provide a better trade-off between throughput and range: LoRaWAN or Sigfox?
- can 5G simultaneously optimize energy consumption in IoT networks and ensure high throughput for critical applications such as train remote control?

A critical challenge related to the questions above is how to deal with the electromagnetic interference (EMI) produced by the recurrent contact losses at the pantograph-catenary interface. Indeed, these communication solutions generally involve antennas placed on or nearby the train's roof so that they may receive the transient EMI produced by the pantograph-catenary contact losses. Furthermore, depending on the intensity of this EMI, the train can even stop [6]. Therefore, resiliency to transient EMI is a key feature for any wireless technology that disputes the competitive railway market. The European Union Agency for Cybersecurity (ENISA) defines resiliency as "The ability of a system to provide and maintain an acceptable level of service in the face of faults (unintentional, intentional, or naturally caused) affecting normal operation" [7]. In this paper, we adopt this definition and we consider fault as the

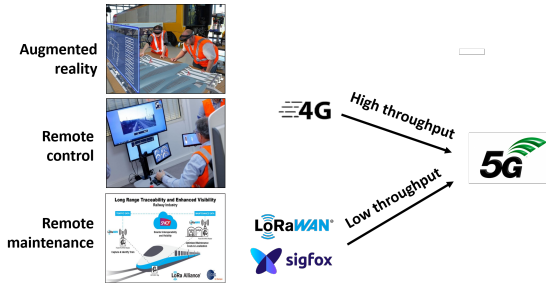

Fig. 1. Some of the new wireless solutions that compete for the railway market and the corresponding throughput demands.

non-intentional transient EMI produced at the pantograph-catenary interface due to contact losses.

In such a scenario, a partnership between two French universities and the French railway company SNCF was established. The referred company is currently modernizing its infrastructure with new wireless solutions. Indeed, some railway operators recently introduced IoT solutions for remote maintenance operations. The goal is to optimize the maintenance of the wagons by making the information about the state of the infrastructure remotely available for the technical staff. Thus, it is no longer necessary to send technicians to the wagons to visually inspect the sensor data. This is part of a digital transformation process that allows the railway industry to adopt predictive maintenance [8]. In this context, SNCF adopted the long-range wide-area network (LoRaWAN) as an IoT communication solution. However, today, other communication technologies such as LTE-M, 5G, and SigFox are proposed to railway operators for IoT applications. Future railway mobile communication systems (FRMCS) have been recently proposed to replace GSM-R as a harmonized standard to allow the interoperability of railway networks based on 5G [9].

Unfortunately, there are no objective assessment methodologies allowing us to compare the susceptibility of these different communication technologies to railway EMI and to select the most appropriate to the railway conditions. Indeed, Mariscotti [10] highlights the need for the update of the railway electromagnetic compatibility (EMC) standards in view of the new digital communication technologies adopted by the electric transportation industry. Classical emissions measurement techniques performed in the frequency domain with quasi-peak or peak detectors do not provide time-domain information of transient EMI, such as the repetition rate [10], [11]. Not considering such information may compromise the susceptibility analysis of communication systems such as the GSM-R, which may be more sensitive to high repetition rates [12]. For this reason, the statistical characterization of transient EMI waveforms in the time domain is being proposed based on amplitude probability distribution (APD) and pulse duration distribution (PDD) [11], [13].

As we can see, the transient EMI produced at the pantograph-catenary interface is still a topic under investigation [14]. More specifically, the immunity of GSM-R [6], [12], [15] and LTE systems [16]–[19] is of particular interest to the railway industry. However, we observed that there is no harmonization in these papers regarding the error indicators used to characterize the immunity of the radio communication systems. A considerable amount of different indicators like bit error rate (BER), [6], [16], block error rate (BLER), [13], error vector magnitude (EVM) [17] and throughput [18] can be found in these studies. Consequently, it can be difficult to compare the robustness of two communication protocols face to transient railway EMI.

Furthermore, certain immunity standards such as the EN 61000-4-4 (used as a reference by the railway standard NF EN 50121-3-2 [20]) suggest the generation of transient voltage pulses, regularly spaced in time, to represent transient EMI phenomena. Consequently, most research papers only focus on regular transient EMI. Nevertheless, a measurement campaign carried out in a French rail in 2012 revealed a highly variable repetition pattern regarding the transient pulses produced by aerial $25\,\mathrm{kV}$, $50\,\mathrm{Hz}$ supply lines [12]. The experimental results in [12] evidence the differences between certain test standard parameters and the real-life transient EMI associated with the catenary-pantograph contact.

This article aims to contribute to the development of a harmonized test methodology to compare different wireless communication systems in terms of resilience to the transient EMI produced by the pantograph-catenary contact. We believe that the harmonized methodology needs to take into account the particular parameters of each communication system (throughput, bandwidth, modulation, symbol time, etc). At the same time, we have to keep in mind that the quality indicators and the error indicators such as BER, BLER, EVM, and acknowledgment (ACK) are not necessarily identical from one communication solution to another. So, the proposed methodology does not necessarily harmonize the indicators but suggests selecting relevant resilience indicators to allow comparisons. It can be helpful for decision-makers in the railway industry when they need to choose one wireless technology among a group of candidates.

To design and evaluate the proposed methodology, we considered two wireless communication systems significantly different, but both employed in railways: LTE and LoRaWAN. We have chosen these two systems because they are based on different communication protocols and modulations, and they serve different applications in the railway domain, requiring different performances. LTE performance is mainly related to the throughput, while LoRaWAN performance is more related to the optimization of power consumption in IoT devices.

The main contributions of the proposed methodology are:

- a transient test waveform that faithfully represents EM transients produced by catenary-pantograph interferences and, at the same time, it is suitable to evaluate the EM susceptibility of different communication systems regardless of the communication channel;
- a comparative analysis involving both regular and irregular repetition intervals between the successive transient test waveforms and the total time duration of the transient sequences. We notably analyze how the regularity or irregularity of time intervals affects the results.
- moreover, given the wide variety of the quality indicators of the different wireless protocols, we propose an upper-level indicator, called the *critical signal-to-interference ratio (SIR)*, which makes it possible to compare susceptibility test results for different communication systems. We notably suggest how to perform a relevant *critical SIR* measurement by taking into account the specificities of the different protocols.

This paper is organized as follows. In Section II, we introduce the LoRaWAN and LTE communication systems, highlighting some use cases in the railway domain. In Section III, we describe the transient EMI phenomenon, and then we specify the main parameters of the EMI waveform. In Section IV, we start to describe our experimental methodology by detailing the test setups, and by highlighting the challenges

to evaluate and compare the two communication protocols. In Section V, we describe the specific error indicators for both communication protocols and the methodology to estimate a generic error indicator (*critical SIR*) during the tests. In Section VI, we present and analyze the main susceptibility results for LoRaWAN and LTE, as well as the repeatability of the results. Finally, we summarize the main findings of this investigation in Section VII.

II. Use of LoRaWAN and LTE systems in the railway domain

In this section, the main characteristics of these communication signals are given after a short introduction to the applications of LoRaWAN and LTE in railways. Indeed, the consideration of the characteristics of the communication signals is essential to define a relevant test methodology.

A. Main applications and coexistence

LoRaWAN is an open protocol managed by LoRa Alliance. However, its physical layer (usually referred to as LoRa) was patented by the Semtech company [21].

The French railway company SNCF adopted an IoT solution based on the LoRaWAN technology to migrate from preventive to predictive maintenance. Before this digital transformation process, the company had to send a group of technicians to the maintenance centers regularly. On these occasions, they verified the state of the wagon's infrastructure by reading the sensor data. Thanks to wireless transmitters connected to these sensors and remote information technology (IT) infrastructure, it is now possible to monitor the state of the trains more frequently and without the need to send the staff to the wagons.

The bridge between sensor nodes and IT infrastructure is made by some gateways installed on the train's roof. The communication between sensors and gateways is established through a LoRaWAN link while gateways communicate with the IT infrastructure using another network (3G/4G/5G, WiFi, Ethernet, fiber-optic or 2.4 GHz radio links [22]).

Different information about the rolling stock can be sent by the sensor nodes to the remote IT infrastructure through the LoRaWAN gateways. Among all this information, we highlight a sensitive one which is the state of the train doors lock systems. In this case, it important to ensure communication reliability despite the presence of transient EMI and other interference sources in the railway environment. Indeed, sensor information is sent to the IT infrastructure, allowing to plan a maintenance action on the door lock system, then the information is transmitted to the on board staff which can check immediately the doors situation.

LTE systems are also present in the railway environment. Currently, they provide internet access to passengers, but in the future, they can also be used for critical operations such as remote train control [5]. In this case, resilience to transient EMI is critical since small packet losses during the communication process can represent the loss of control over the train movements. This can, in turn, compromise the safety of the passengers.

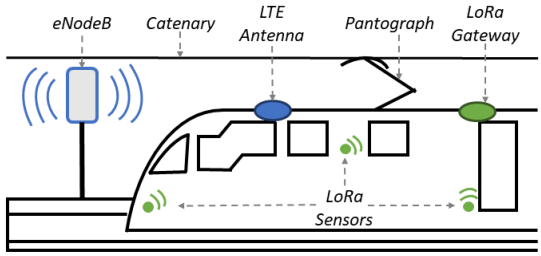

(a)

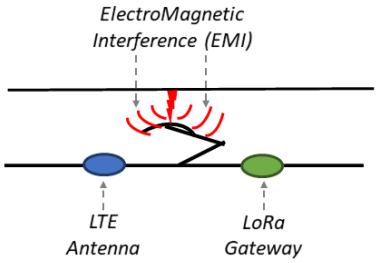

(b)

Fig. 2. (a) Coexistence of LoRaWAN and LTE networks in the railway environment. (b) Occurrence of an electric arc at the catenary-pantograph interface, in close proximity to the communication antennas.

For the proper operation of both LoRaWAN and LTE systems, they must be resilient to EMI. The coexistence of these two communication systems within a wagon is illustrated in Fig. 2(a) and the occurrence of an electric arc at the catenary-pantograph interface with subsequent irradiation of transient EMI is illustrated in Fig. 2(b).

As we can see in Fig. 2(b), both LTE antenna and LoRaWAN gateway are installed on the roof of the train and therefore both are physically close to the electric arc phenomenon. The reason why the LoRaWAN gateway is installed on the roof is that although it receives signals from the sensors which are installed inside the train, it also needs to forward the sensor data to a remote IT infrastructure. To do so, gateways normally use public networks such as LTE to access the remote servers. Therefore, the exposition to the transient EMI is unavoidable. Consequently, the gateway receiving antenna will eventually receive a combination of sensor data (LoRa uplink signals) and transient EMI.

B. Physical layer parameters

1) LoRaWAN: LoRa is based on the chirp spreading spectrum (CSS) modulation technique and on a time-division duplex (TDD). In Europe, the transmitting frequencies of the EU868 band are defined within the range from 863 MHz to 870 MHz. Long communication ranges can be achieved at the cost of throughput. A trade-off can be established through a parameter called spreading factor (SF), which ranges from 7 (smallest range, highest throughput) to 12 (most extended range, lowest throughput). This parameter defines the constellation size, which is constrained to 2^{SF} symbols. The SF can be manually or automatically set by enabling the adaptive data rate (ADR). In our tests, we adopt an SF of 12, and we do not enable ADR. These conditions ensure

more repeatable results. The transmitting frequency is set to $868.3\,\mathrm{MHz}$.

Another configurable parameter is the coding rate (CR). It defines the proportion of error-correction bits included in a data frame. These are the four possible CR values in LoRa: $4/5, 4/6, 4/7, 4/8$. During our tests, we adopted a $\mathrm{CR} = 4/5$, meaning that for each 5 transmitted bits, 4 are useful bits and 1 is an error-correction bit, *i.e.* 20% of the transmitted bits are used by the receiver to verify the integrity of the received data. This value was adopted because it represents the worst-case scenario in terms of EM susceptibility (in $\mathrm{CR} = 4/8$, for example, there are 50% of error-correction bits).

Finally, the allowed LoRa bandwidths are: $125\,\mathrm{kHz}$, $250\,\mathrm{kHz}$ and $500\,\mathrm{kHz}$. Higher bandwidths allow higher throughput but the number of users sharing the spectrum decreases. In this work, we adopt a bandwidth of $125\,\mathrm{kHz}$ [23].

2) LTE: On the other hand, LTE allows both TDD and frequency-division duplex (FDD), and it is based on the quadrature phase-shift keying (QPSK) and the quadrature amplitude modulation (QAM) schemes. LTE channels are distributed along different frequency bands within the $410\,\mathrm{MHz}$ to $5900\,\mathrm{MHz}$ range. In this work, we adopt Band 8, which reserves the $880\,\mathrm{MHz}$ to $915\,\mathrm{MHz}$ band for uplink (UL) and $925\,\mathrm{MHz}$ to $960\,\mathrm{MHz}$ for downlink (DL). The allowed channel bandwidths are: $1.4\,\mathrm{MHz}$, $3\,\mathrm{MHz}$, $5\,\mathrm{MHz}$, $10\,\mathrm{MHz}$, $15\,\mathrm{MHz}$ and $20\,\mathrm{MHz}$. We adopted the QPSK modulation and $20\,\mathrm{MHz}$ LTE channels in our tests.

LTE is based on orthogonal frequency-division multiplexing (OFDM). In LTE, the subcarrier frequencies are spaced by $15\,\mathrm{kHz}$ with a symbol time of $66.7\,\mu\mathrm{s}$. One LTE subframe includes 14 symbols for a total duration of $1\,\mathrm{ms}$. Ten LTE subframes compose an LTE frame [24].

The choice we made of adopting LTE Band 8 is due to its proximity with the EU863-870 band, which is used for LoRaWAN transmissions in Europe. Such a choice facilitates the comparison between the results regarding the two communication technologies. In particular, in the next section, we introduce a transient interference model whose envelope is preserved for both LTE and LoRaWAN studies, thanks to the proximity of the frequency bands.

3) Summary: Table I summarizes LoRaWAN and LTE main physical layer parameters. One remarkable difference is the throughput, which is much lower in LoRaWAN than in LTE. It means that, while LoRaWAN is normally used to send punctual information about the rolling stock from time to time to SNCF, LTE is expected to ensure the real-time transfer of large amounts of data. Another difference is the fact that LoRaWAN adopts time-division duplexing (TDD) while LTE allows both TDD and frequency-division duplexing (FDD). In this work, we adopt FDD for LTE.

III. Interference produced by the pantograph-catenary contact

In the previous section, we briefly introduced the EMI produced by the catenary-pantograph contact (see Fig. 2(b)). Now, we give more details about the physical phenomenon behind this interference. We also introduce a mathematical model and the corresponding parameters, *i.e.* rise time, transient duration, sequence duration, central frequency, and the interval between transients.

A. Physical phenomenon and mathematical modeling

In a normal situation, the electric system of the train is continuously fed by an external supply line through the pantograph-catenary contact. However, disconnections can occasionally happen when the train moves over the rail. Such disconnections can, in turn, produce electric arcs such as those illustrated in Fig. 2(b). Due to their short duration (usually, a few tens of ns), the spectral content of the resulting EM radiation can overlap the LoRaWAN and LTE frequency bands, and therefore it can be sensed by the respective receiving antennas, reaching the LTE user equipment (*e.g.* a WiFi router) and the LoRaWAN gateway. Therefore, the EMI will mainly affect the LoRaWAN uplink signals (LoRaWAN end device $\rightarrow$ gateway) and the LTE downlink signals (eNodeB $\rightarrow$ LTE user equipment), eNodeB being the base station.

Figure 3 shows one transient EMI sequence measured on board a train with an oscilloscope connected to the GSM-R antenna [12]. To perform the such measurement, authors in [12] directly connected an oscilloscope to a GSM-R antenna installed on the roof of the train. Therefore, no amplification or attenuation was employed to detect the amplitude of the transient EMI. The GSM-R antenna used in this measurement campaign was found to have an operating frequency band ranging from $780\,\mathrm{MHz}$ up to $1\,\mathrm{GHz}$ [25]. The behavior of each transient can, in turn, be described based on the rise time (RT) and the transient duration (TD). These two waveforms show that the interval between two consecutive transients is highly variable.

Such variability can be explained by the electrical and mechanical parameters involved in the physical phenomenon of an electric arc at the pantograph-catenary interface. According to [12], the conductivity of the sliding contact, which is influenced not only by the constituent material but also by other factors such as the ruggedness of the surface and oxidation, can play a role in the electric arc emissions. Furthermore, it is also necessary to take into account the external conditions (*e.g.* temperature and humidity), the train speed, and the mechanical characteristics of the catenary system, among other parameters. There is, therefore, a huge amount of factors that shape the transient waveform, whose resulting dynamics are highly variable.

To know which RT and TD values are more common in practice, authors in [12] performed several measurements, which allowed them to derive corresponding statistical distributions. They found out that the RT and TD values are usually in the order of magnitude of a few units of ns and a few tens of ns, respectively. Once the RT and TD values are available, we use the following double exponential model to generate one transient pulse [6]:

$$\mathrm{S(t)} = \mathrm{A} \times (\mathrm{e}^{(-1/\mathrm{TD})\mathrm{t}} - \mathrm{e}^{(-1/\mathrm{RT})\mathrm{t}}) \times \mathrm{U(t)} \times \sin(2\pi \mathrm{Ft}), \tag{1}$$

TABLE I
LoRaWAN and LTE physical layer parameters

Protocol	Duplexing method	Modulation	Spreading factor	Coding rate	Throughput (kbps)	Bandwidth	Reference
LoRaWAN	TDD	CSS	12	4/5	0.3 – 5	125 kHz	[23], Section 2.4.2, Table 6
LTE	FDD	QPSK	N/A	1/3	1107.2	20 MHz	[24], Page 6238, Table A.3.2-1h

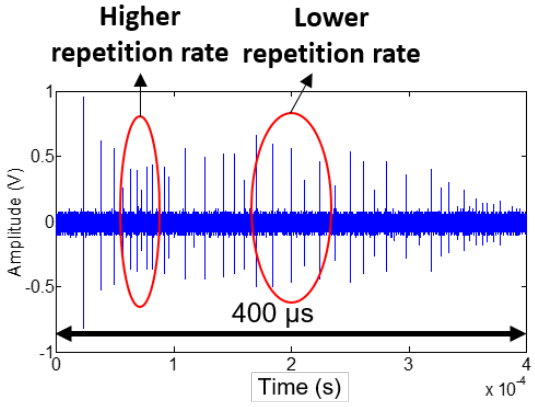

Fig. 3. Transient EMI waveform measured by a GSM-R antenna [12]. In this figure, we highlight the irregularity of the transient sequence.

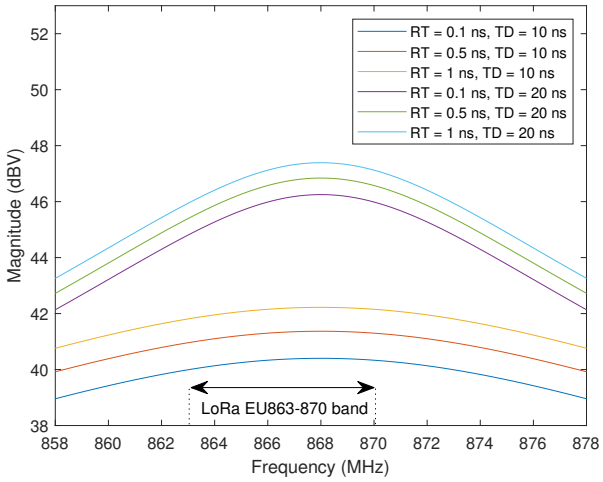

Fig. 4. Magnitude spectra of unitary transient pulses with different rise times and transient durations.

where A is the amplitude, U(t) is the unit step function, and F is the carrier frequency. In our experiments, we adopt F = 868 MHz for the LoRaWAN tests and F = 942 MHz for the LTE tests. The carrier frequency is an important parameter in our test methodology because it allows us to generate only the EMI spectral components seen by the input filters of the LoRaWAN gateway and the LTE user equipment. Consequently, the amount of power required from the signal generator is reduced, thus avoiding the test equipment being exposed to high levels of EMI. Finally, we highlight that Eq. (1) ensures that the EMI waveform will always follow the same behavior. Therefore, establishing a mathematical model contributes to the repeatability of the test methodology.

B. Rise time and transient duration

We consider the Fourier transform of a single transient to define the most suitable RT and TD. In Fig. 4, we superpose the spectra of transient interference with different RT and TD, considering a 20 MHz bandwidth around 868 MHz and thus covering the EU863-870 LoRaWAN frequency band (alternatively, we could have chosen a central frequency based on an LTE commercial band).

The RT values in this figure are less or equal to 1 ns and the TD values are inferior to 50 ns, which correspond to typical parameters of transients measured on-board trains [12]. Among all the curves shown in Fig. 4, we choose the yellow one (RT =1 ns, TD =10 ns) for two reasons. First, because it is almost flat so the EMI effects on the LoRa receiver are the same no matter which transmission channel was chosen for the test. This is not true for the three curves in Fig. 4 corresponding to TD =20 ns. Such characteristics can be particularly useful if frequency hopping is enabled. And second, because it demands less power or amplification to be generated in comparison to RT =0.1 ns, TD =10 ns (blue curve) and RT =0.5 ns, TD =10 ns (red curve).

In summary, our goal is to define an EMI spectrum that is both flat and has the maximum possible associated power. By doing so, we avoid disturbing certain communication channels more than others, and at the same time less amplification is required to generate it. Among the 6 options shown in Fig. 4, the combination RT =1 ns, TD =10 ns is the option that best serves this purpose.

C. Interval between transients and sequence duration

In this work, we consider both regular and irregular time intervals between transients with average values equal to 5 µs. This average interval between transients is coherent with the measurements reported in [12]. Furthermore, the comparison between regular and irregular transient sequences was not explored in similar studies such as [15], which only report the effects of regular transient EMI sequences.

Following basic signal processing principles, we can say that when the interval is regular, the spectrum of the resulting sequence is simply a sampled version of those illustrated in Fig. 4. In this case, the distance between two frequency components is inversely proportional to the time interval between transients. Consequently, the spectral components of the 5 µs regular sequence are 200 kHz apart from each other.

However, the spectrum of the transient sequence becomes less homogeneous when the interval is irregular. This can be explained by the fact that random frequencies are generated when the interval between transients is random. If we create

longer sequences, more frequencies are generated; therefore, the spectrum becomes more homogeneous, reducing thus power oscillations between successive LoRaWAN and LTE communication channels. In this work, we generate sufficiently long transient EMI sequences so we can consider that they are channel-independent.

In similar studies, authors normally use relatively complex test benches to generate electric arcs which, in turn, result in transient EMI [14], [15], [26]. One disadvantage of these methods is that the EMI waveform parameters like RT, TD, and repetition rate are controlled by physical phenomena generated in the laboratory and, therefore, subject to imprecisions of the test bench. For example, in [15], authors create transient sequences by using an electrostatic discharge (ESD) generator and a metallic surface. The regularity of the transients is proportional to the distance between the ESD generator and the metallic surface. Therefore, any small imprecision related to the test bench can compromise the accuracy of the repetition rate.

Our method, on the other hand, allows us to have more control over these parameters, once the sequence is created in MATLAB and then uploaded on an arbitrary signal generator. To do that, we generate a sequence of 100 transients within a time interval of $500\,\mu s$, where the length of this sequence is limited by the equipment memory. The time interval between transient pulses is random but an average interval of $5\,\mu s$ is preserved. Once this sequence is loaded on the arbitrary signal generator, it starts to be transmitted continuously.

To design the transient sequences, we use MATLAB. Here, we explain how we generate sequences with irregular intervals. First, we generate a single transient pulse based on Eq. 1. Then, we randomly position a predefined number of transient pulses within a given time interval (*e.g.* 100 transients within a $500\,\mu s$ interval to form an irregular sequence with an average interval between transients of $5\,\mu s$). The precise time instant where a transient pulse takes place is defined by a continuous uniform distribution whose argument ranges from $0\,\mu s$ up to $500\,\mu s$.

D. Transient EMI according to the EMC standards

Telecommunication standards normally define performance criteria for communication systems without any particular remark about the environment where they are installed. Railway standards, on the other hand, specify transient immunity test parameters to test radio equipment installed on board trains. Both the railway EMC standard EN 50121-3-2 [20] and the EMC standard ETSI EN 300 386 [27] devoted to telecommunication network equipment make reference to the immunity standard EN 61000-4-4 which is applicable to a broad range of electronic devices. In both EN 50121-3-2 and ETSI EN 300 386, the transient EMI sequence has a fixed repetition frequency. In this work, we evaluate transient EMI sequences with fixed and non-fixed repetition frequencies.

IV. Test setup

Now that the communication signals (LTE and LoRaWAN) and the transient EMI waveform are characterized, we can detail our test setup. Our test bench allows us to use different proportions to combine the communication signal and EMI power. This procedure will enable us to simulate different EMI severity levels, which, in practice, depend on several factors, such as the train's speed and the location of the communication antennas.

A. General principles

The proposed test benches allow us to simultaneously generate useful communication signals and transient EMI, then combine these two waveforms in such a way as to cover a specific SIR range and finally monitor the data communication. The data communication can be established and monitored using the same devices of real communication networks or laboratory equipment that emulate uplinks and downlinks. On the other hand, the interference can be generated based on Eq. (1) and with the aid of an arbitrary signal generator. Finally, the connection between all these devices can be established with wires or antennas. Our work is based on conducted test benches. Such an approach is useful for a first evaluation of the EM susceptibility of a communication system where we only analyze the effects of transient EMI. However, it can be pertinent to establish wireless links in a second moment to evaluate the communication system in a more realistic scenario. The conducted test benches used in our investigation are illustrated in Fig. 5. Figure 6 shows the coaxial and power terminals of the gateway and LTE user device.

In Figs. 5(a) and 5(b), two splitters are used to combine the communication signals with the interference. A variable attenuator is used to reduce the communication signal power and, therefore, to control the SIR. The idea is to start the test with a high SIR level and progressively reduce it until communication errors occur.

B. Equipment used

Performing test on LoRaWAN or LTE communications requires using specific communication terminals dedicated to each protocol. Figure 5(a) is an illustration of the LoRaWAN test setup. We use an SX1276 transceiver, a Kerlink iFemto-Cell gateway, a Raspberry web server, and the open-source network server ChirpStack. With ChirpStack, we can check the values of certain physical layer (PHY) parameters, such as the received signal strength indicator (RSSI) and the signal-to-noise ratio (SNR). Besides, ChirpStack allows us to check if each uplink message is followed by a corresponding acknowledgment (ACK) message. The absence of ACK messages indicates a critical situation, as detailed in Section V-A1. Finally, the SIR is controlled thanks to a J7211A attenuator.

The LTE test setup is shown in Fig. 5(b). A CMW500 radio communication tester plays the role of eNodeB, and an LTE dongle is used as the user device. The LTE downlink power levels are progressively reduced thanks to a Phyton routine that remotely accesses and automatically controls the radio communication tester. Once we launch this routine, a report containing the pre-programmed power levels and the corresponding BLER levels is generated.

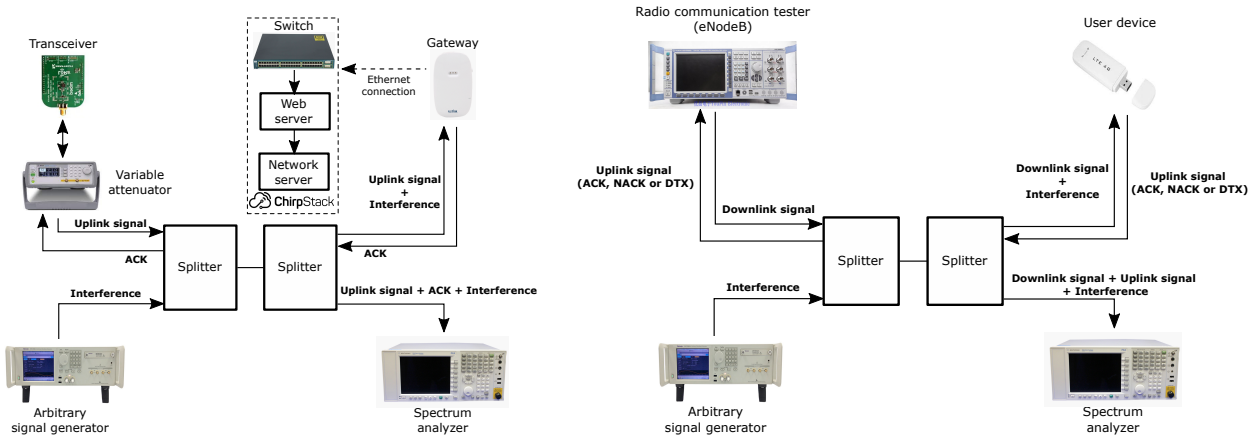

(a) (b)

Fig. 5. Illustration of the test benches. (a) LoRaWAN. (b) LTE.

(a) (b)

Fig. 6. Illustration of the power supply and coaxial connections. (a) Gateway. (b) LTE user device.

In both LoRaWAN and LTE test setups, an AWG70001A arbitrary signal generator and an N9030A PXA spectrum analyzer are used. They allow us to generate the interference and calculate the SIR, respectively. In the LoRaWAN test setup, the spectrum analyzer is also used to monitor the ACK signal. Like this, it serves as a complement to ChirpStack.

The SIR control is achieved in our tests with a progressive decrease of the LoRaWAN and LTE uplink and downlink power levels, respectively. Due to the differences between the LoRaWAN and LTE test equipment, we adopted different strategies to control the transmission power. While the LoRa transceiver is a simple device with multiple applications, the CMW500 is a measurement equipment used by the telecommunication industry to test radio devices by emulating base stations. In view of these differences, we needed to use an external attenuator to control the LoRa uplink power. However, this was not necessary for the LTE test bench, since the CMW500 allows the user to define the desired transmission power.

Still, we checked the power levels of the signals emitted by the CMW500. To do so, we connected the CMW500 directly to the spectrum analyzer using a short cable. We realized with this verification procedure that the equipment was indeed generating power according to the value chosen by the user.

V. Error Indicators and Critical SIR

The test bench detailed in the previous section allows us to generate different communication signal power and EMI power combinations, *i.e.* different signal-to-interference power ratio (SIR) levels. However, we are mainly interested in finding which are the *critical SIR* values. The critical SIR represents a situation where the EMI power is sufficient to impact communications. However, we first need to define communication error indicators before calculating it. This is one of the main obstacles to harmonizing the test methodology due to the different nature of the protocols.

In this section, we propose a critical SIR calculation based on two parameters: acknowledgment (ACK) for the LoRaWAN system and block error rate (BLER) for the LTE system. These are key parameters related to the LoRaWAN and LTE protocols. Indeed, real LoRaWAN and LTE devices compute such parameters; they use them to evaluate the reliability of data communication and to define countermeasures. For example, we observed during our experiments that, if the LoRa receiver does not identify the presence of an ACK, it immediately reduces the interval of time between two successive uplink signals. Therefore, it sends more data for the same interval of time, in an attempt to re-establish communication with the gateway.

In most cases, however, it is difficult or even impossible

to employ the same performance or immunity indicators for different communication systems. Indeed, according to the communication solution, we cannot measure or estimate the same indicators. For example, BLER is an accessible and relevant indicator for LTE. A closed-form expression for the BLER is specified in the 3GPP standard, which also defines a critical value of 5% [24, p.202]. However, the BLER cannot be obtained for LoRaWAN. Indeed, in the LoRaWAN protocol, the LoRa demodulation directly extracts full symbols and no BLER estimation method is defined. Taking into account the whole LoRaWAN protocol (and not only the LoRa modulation), the only indicator accessible is the presence or the absence of ACK.

A. Error indicators

The error indicators to which we have access can be very different depending on the communication protocols. This is due to differences in modulation and network configuration, resource access rules, or the proprietary nature of the protocol.

1) LoRaWAN: LoRaWAN features an acknowledgment (ACK)-based protocol, which can be explained as follows. The end device sends a message (uplink) to the gateway. The gateway generates an ACK signal if the uplink message is correctly received. If the received message is corrupted, the gateway generates no ACK signal. This mechanism is illustrated in Fig. 7.

In the LoRaWAN protocol, there are three A, B, and C device classes. The processes illustrated in Fig. 7 refer to Class A end devices. Such devices present minimum energy consumption compared to Classes B and C since receivers do not try to decode the received signal all the time but only during specific time intervals. We employed Class A end devices due to the ACK feature allowing to identify communication problems caused by transient interference.

Since we use a Class A device, two-time windows are reserved for the reception of the ACK signal. These time windows are defined by two configurable parameters called RX1 Delay and RX2 Delay, as illustrated in Fig. 7. They are described in time units, having as a reference the time instant where the transmission of an uplink frame finishes. If we observe how both uplink and ACK signals evolve over time, we can identify anomalies occurrences.

We, therefore, configure the spectrum analyzer illustrated in Fig. 5(a) in the zero-span mode. When configured in this mode, the spectrum analyzer shows how the signal power seen through a band-pass filter (in this case, with a resolution bandwidth of $125\,\mathrm{kHz}$) evolves with time. Given the nature of the process illustrated in Fig. 7, the signal power is most of the time negligible, except when there is data exchange. Power peaks with short duration reveal the presence of uplinks and ACKs. These signals appear in pairs, meaning communication is lost when this pattern is not observed.

2) LTE: LTE systems also include an ACK-based protocol, as illustrated in Fig. 8. This figure shows that in a normal situation (*i.e.* no EMI), for each LTE subframe received by the user equipment, one ACK signal is sent to the eNodeB. However, in the presence of EMI with sufficient power to disturb the LTE communications, some of these subframes may be corrupted and sometimes not even detected by the user equipment. In the first case, the user equipment generates a non-ACK (NACK); in the second situation, the eNodeB generates a discontinuous transmission (DTX).

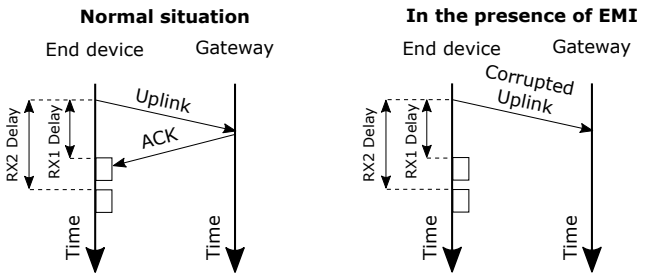

Fig. 7. Message exchange between a Class A LoRaWAN end device and a gateway, with and without EMI. The two rectangles on the end device timeline represent time windows dedicated to the reception of the ACK message.

By defining $\mathrm{n_{ACK}}$, $\mathrm{n_{NACK}}$ and $\mathrm{n_{DTX}}$ as counters which respectively quantify the total number of ACKs, NACKs, and DTXs registered by the eNodeB during a specific time interval, a block error rate (BLER) can be calculated as follows:

$$\mathrm{BLER} = \frac{\mathrm{n_{NACK}} + \mathrm{n_{DTX}}}{\mathrm{n_{ACK}} + \mathrm{n_{NACK}} + \mathrm{n_{DTX}}}. \tag{2}$$

Equation 2 indicates that both situations described above (corrupted or non-received LTE downlink messages) contribute to the increase of the BLER. In this work, we use the BLER as the LTE error indicator.

B. Critical SIR

1) Definitions: Here, we define what a critical situation is.

- LoRaWAN: once an ACK is lost due to the EMI, the end device starts to generate a series of uplink messages in an attempt to recover the communication with the gateway. So, we define the critical situation as the first missing ACK. However, we observed during the experiments that sometimes the communication can be recovered after a specific time, while sometimes the communication is permanently lost. We will highlight these two scenarios when exposing the experimental results.
- LTE: the LTE error analysis is based on a 5% BLER tolerance margin, as specified in the 3GPP standard [24, p.202].

To sum up, the critical situation is defined as the absence of ACK for LoRaWAN and the BLER threshold of 5% for LTE. The critical SIR is the SIR for which the critical situation happens. We will explain in the next section the SIR measurement methodology.

2) Methodology to measure the critical SIR: The first step to measure the critical SIR is to separately measure the communication signal and interference power without any attenuation before the test. The communication signals of interest are the LoRa uplink signal and the LTE downlink signal (see Figs. 5(a) and 5(b)).

So, before the LoRaWAN test, we turn on the transceiver and the gateway while we set the attenuator to $0\,\mathrm{dB}$, and we

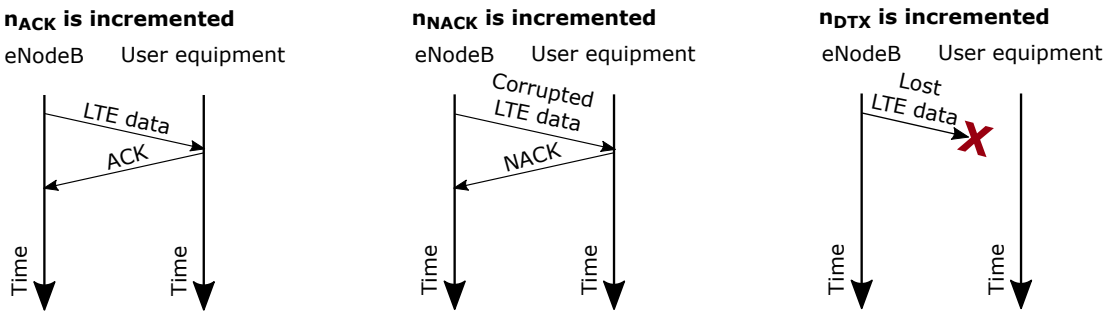

Fig. 8. Message exchange between eNodeB and an LTE user equipment. Left: normal situation. Center and right: in the presence of EMI. This figure illustrates how the counters used in the BLER calculation are incremented.

turn off the signal generator. Similarly, before the LTE test, we turn on the radio communication tester and the user device while we turn off the signal generator. By doing so, we have the reference power levels of the two communication signals.

In a second moment, we turn off the communication systems while we turn on the signal generator. The signal generator is first loaded with a regular transient EMI sequence and then with an irregular one. This procedure allows us to have the reference power levels of the interfering signals.

Now that we have the communication and interfering signals' reference power levels, we start the test by turning on the communication system (either LoRaWAN or LTE) and the signal generator simultaneously. The attenuator is initially set to $0\,\mathrm{dB}$, but the attenuation level is progressively increased with a $1\,\mathrm{dB}$ step. When a critical situation is observed, we stop the test, and we calculate the critical SIR as follows:

$$\mathrm{SIR}_{\mathrm{critical}}[\mathrm{dB}] = \mathrm{P}^{\mathrm{com}}_{\mathrm{critical}} - \mathrm{P}^{\mathrm{EMI}}, \tag{3}$$

where $\mathrm{SIR}_{\mathrm{critical}}$ and $\mathrm{P}^{\mathrm{com}}_{\mathrm{critical}}$ are the critical SIR and the corresponding power level of the communication signal. For the LoRaWAN test, $\mathrm{P}^{\mathrm{com}}_{\mathrm{critical}}$ equals to $(\mathrm{P}^{\mathrm{0dB}}_{\mathrm{com}} - \mathrm{att}_{\mathrm{critical}})$, where $\mathrm{P}^{\mathrm{0dB}}_{\mathrm{com}}$ is the communication signal power measured with the signal generator turned off and the variable attenuator set to $0\,\mathrm{dB}$ and $\mathrm{att}_{\mathrm{critical}}$ is the critical attenuation. Finally, $\mathrm{P}^{\mathrm{EMI}}$ is the EMI power measured with the communication system turned off.

The power measurements were performed with an Agilent PXA N9030A signal analyzer configured with the *channel power* mode. This measurement allows us to know the approximate EMI power level seen by LoRaWAN and LTE radio receivers. To proceed like that, we first define the central frequency of the communication channel ($868\,\mathrm{MHz}$ for LoRaWAN and $942\,\mathrm{MHz}$ for LTE).

Proceeding with the spectrum analyzer configuration, we define a sufficiently large span that allows us to visualize all the communication channels (in this work, we used a span of $20\,\mathrm{MHz}$); the resolution bandwidth and a parameter called *integration bandwidth*, both playing the role of the radio receiver input filter; and the sweep time, which plays the role of the time window used by the radio receiver to read the received signal. To measure the LoRaWAN channel power, we defined a resolution bandwidth of $130\,\mathrm{kHz}$ and an integration bandwidth of $125\,\mathrm{kHz}$. On the other hand, to measure the LTE channel power, we defined a resolution bandwidth of $15\,\mathrm{kHz}$ (equivalent to the separation between two LTE subcarriers) and an integration bandwidth of $20\,\mathrm{MHz}$. All these parameters are based on LoRaWAN and LTE radio receiver specifications. We adopted a sweep time of $1\,\mathrm{ms}$.

Attention must be taken when measuring the power of communication signals based on TDD, such as LoRaWAN. In this case, uplink and downlink signals occupy the same frequency band. Consequently, if we configure the spectrum analyzer to use peak or average detectors, the power measurement can be biased by the superposition of uplink and downlink signals.

In summary, we measure the impact of the transient EMI based on the average interference power within a LoRaWAN/LTE communication channel at the moment where the communication starts to be affected. The proposed methodology is faster than the one we proposed in [28], which demands post-processing. Besides, only one communication system was investigated in [28], so the harmonizing nature of this indicator was not yet explored.

VI. Results

This section presents the effects of transient EMI over LoRaWAN and LTE systems. We explore these two communication systems separately. For each test configuration, we repeated the procedure 10 times to more clearly observe the communication systems' behaviors in the presence of interference and to take into account possible variability in test results. All test results are presented in terms of critical SIR levels.

The experimental analyses are focused on the comparison between the impact of regular and irregular intervals between successive transients. Regular transient interference intervals represent the typical waveforms suggested by most EMC immunity standards while irregular transient interference intervals represent realistic behaviors in view of the experimental/statistical results present in [12].

Figures 9 and 10 show, respectively, the critical SIR levels of the LoRaWAN and LTE systems in the presence of transient EMI pulses, either regularly or irregularly spaced in time, and with an average time interval of $5\,\mu\mathrm{s}$. Furthermore, each critical SIR level is associated to one of these three groups, according to the effects caused to the communication system:

- Communication re-established: the receiver does not respond with ACKs to the UL messages sent by the

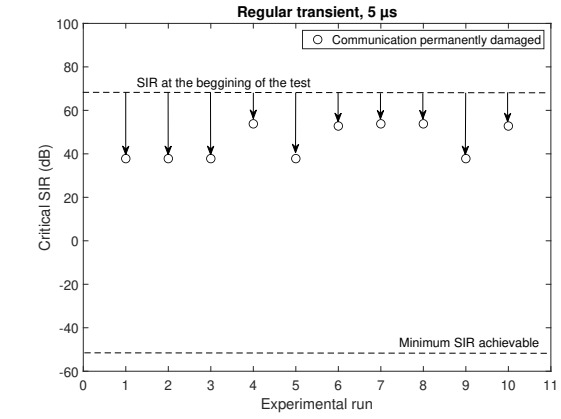

(a)

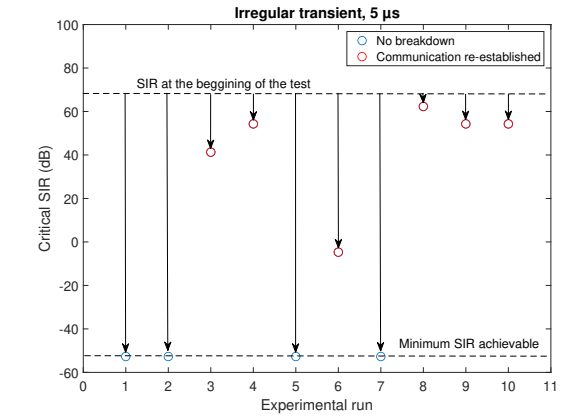

(b)

Fig. 9. Critical SIR levels of LoRaWAN systems in the presence of a series of transient EMI pulses, (a) regularly or (b) irregularly spaced in time, and with an average time interval of 5 µs.

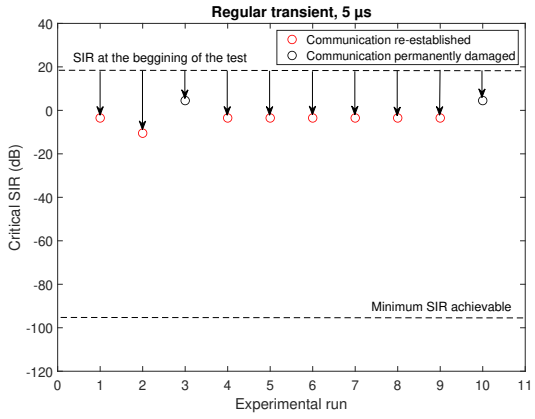

(a)

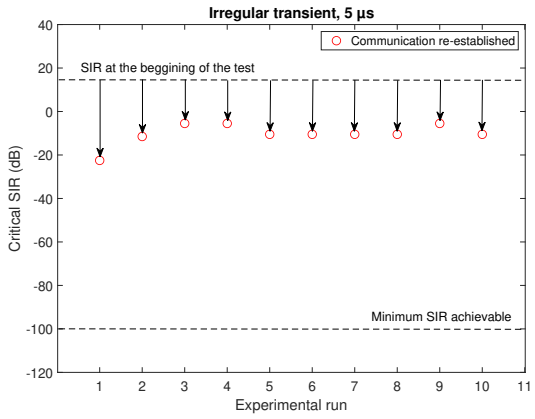

(b)

Fig. 10. Critical SIR levels of LTE systems in the presence of a series of transient EMI pulses, (a) regularly or (b) irregularly spaced in time, and with an average time interval of 5 µs.

transmitter during a short period but the communication is reestablished after a while despite the presence of EMI.

- Communication permanently damaged: the receiver stops responding with ACKs to the UL messages sent by the transmitter and the communication is not reestablished unless we remove the interference.
- No breakdown: the presence of EMI does not affect the exchange of UL and ACK messages even under the minimum SIR level achieved with the test equipment.

A. *Interpreting the results*

1) LoRaWAN: A comparison between Figs. 9(a) and 9(b) reveals that the regularity of the transient EMI sequences plays an important role in the impact of the interference on the LoRaWAN system. From Fig. 9(a), it is clear that the LoRaWAN system can be very sensitive to transients occurring with regular intervals, reaching critical SIR levels as high as 60 dB. Besides, communication was permanently lost in most cases, meaning there was no ACK even after the removal of the EMI.

On the other hand, Fig. 9(b) reveals a different behavior. In 60% of the cases, communication was re-established a few seconds after the first ACK was lost. So, despite the corresponding high critical SIR levels and a few messages lost, the communication showed certain robustness against this type of interference. Besides, 4 out of 10 measurements lie in a very low critical SIR zone in Fig. 9(b). In this zone (labeled as *no breakdown* in this figure), the communication was not lost even with very low SIR levels. The test was stopped when the attenuation applied to the LoRa transmitter reached 121 dB (the limit of the attenuator used in the tests).

The first step to interpreting these results is to understand the difference between the characteristics of the EMI produced by the pantograph-catenary contact and the characteristics of the EMI which is actually observed at the input of a LoRa or an LTE radio receiver. Once a signal is detected by the radio receiver, several operations such as filtering, sampling, analog-to-digital conversion, and fast Fourier transform (FFT) are applied. Consequently, the EMI characteristics after all these stages may differ from those produced by the interference source. Furthermore, the filter, sampling, and FFT parameters may change from one radio receiver to another, depending on the communication technology. So, it is possible that a LoRa receiver and an LTE receiver process in different ways the same EMI.

To check that, let us first analyze Fig. 11. This figure illustrates how the transient EMI waveforms considered so far (regular and irregular with an average interval of 5 µs)

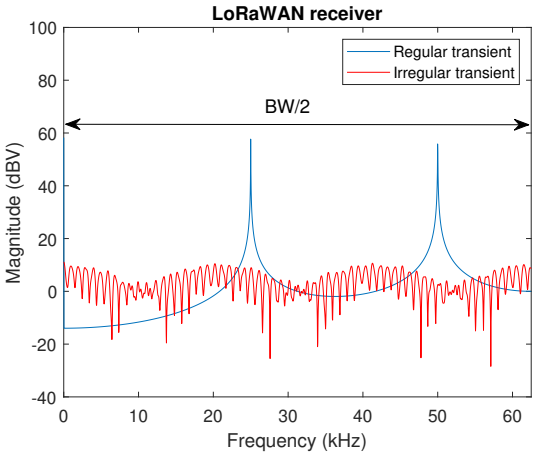

Fig. 11. Transient EMI unitary sequences seen, in baseband, by a 125 kHz LoRaWAN receiver with the following FFT parameters: a 32.8 ms duration, a 30.5 Hz frequency resolution, and a 125 kS s^{-1} sampling frequency. Average interval between transients: 5 µs.

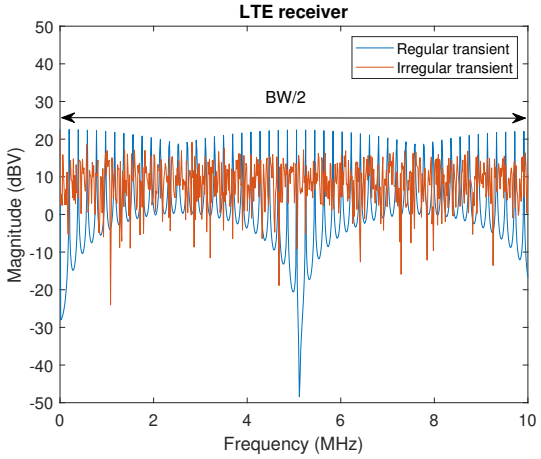

Fig. 12. Transient EMI unitary sequences seen, in baseband, by a 20 MHz LTE receiver with the following FFT parameters: a 66.7 µs duration, a 15 kHz frequency resolution, and a 30.72 MS s^{-1} sampling frequency. Average interval between transients: 5 µs.

TABLE II
FFT PARAMETERS.

Protocol	Duration	Frequency resolution	Sampling frequency
LoRaWAN	32.8 ms	30.5 Hz	125 kS s^{-1}
LTE	66.7 µs	15 kHz	30.72 MS s^{-1}

are actually seen by a LoRaWAN receiver configured with SF = 12 and with a bandwidth of 125 kHz. These waveforms were obtained by applying an FFT to these sequences with the parameters indicated in Table II, first line. The time duration of the FFT is, in this case, 32.8 ms, which corresponds to the symbol time of the LoRaWAN receiver. Combined with the sampling frequency of 125 kS s^{-1}, this time duration leads to a frequency resolution of 30.5 Hz.

Figure 11 reveals that, while the energy of the regular transient sequence is concentrated around specific frequencies, the irregular sequence spectrum is more homogeneous. Therefore, the irregular transient sequence is more likely to be identified as white noise by the LoRaWAN receiver. In other words, in most cases, the irregular transients do not cause symbol errors during the LoRa demodulation process. We believe that this explains the very low critical SIR results, close to −50 dB, presented by the irregular sequences (see Fig. 9(b)). This could also explain why in most cases, the communication is re-established after a few seconds when submitted to the irregular disturbances while it is permanently damaged when submitted to the regular disturbances. On the other hand, the regular transients can affect the LoRa demodulation process and cause symbol errors due to their energy distribution, which resembles more a communication signal than white noise.

2) LTE: A similar analysis was applied to LTE. Figure 12 shows how a typical LTE receiver interprets a regular and an irregular transient sequence with an average interval of 5 µs. The FFT parameters can be seen in Table II, second line. The FFT duration is 66.7 µs, corresponding to an LTE symbol time. This value, combined with a sampling frequency of 30.72 MS s^{-1}, results in a frequency resolution of 15 kHz.

Results shown in Fig. 12 indicate that the regular transient spectrum has more energy on certain sub-carriers within the LTE channel bandwidth than the irregular one. This could explain why the critical SIR levels associated with the irregular transient sequence are lower than those associated with the regular transient sequence (compare Figs. 10(a) and 10(b)).

Let us compare Fig. 11 with Fig. 12. We see that the difference between the regular and the irregular sequence spectra is more intense for the LoRaWAN receiver than the LTE receiver. Indeed, the discrepancy between the critical SIR levels of regular and irregular sequences can be as high as 100 dB for the LoRaWAN receiver (compare Figs. 9(a) and 9(b)), while this discrepancy falls to approximately 5 dB for the LTE receiver (compare Figs. 10(a) and 10(b)).

However, we must consider the application assigned to each communication system to interpret these susceptibility results. Indeed, regarding the applications provided by the LTE, they require a permanent minimum level of robustness to ensure internet access or control remote train driving. On the other hand, the applications provided by LoRaWAN consist in punctually sending sensor data to IoT platforms. So, for the LoRaWAN, if a short message is systematically repeated several times, we can consider that the IoT platform will receive the message (statistically speaking, due to the variability of the critical SIR measured). It may be necessary to adapt how results are analyzed, especially when testing resource and energy-efficient protocols.

B. Interference spectra at the input of the LTE and LoRaWAN receivers

To calculate the spectra shown Figs. 11 and Fig. 12, we first generate a baseband version of Eq. 1. We discard the sine term of this equation, conserving only the envelope of the double exponential. As a consequence, the frequency components of such signal range from -BW/2 Hz up to BW/2 Hz, where BW is the signal bandwidth. Given the symmetry of the baseband signal around 0 Hz, we only show half bandwidth in Figs. 11

and Fig. 12. This process is equivalent to the down-conversion from the modulation band to the intermediary frequency in commercial radio receivers.

To preserve the envelope shape, a high enough sampling rate is used to generate the transient EMI sequence in the first instant. However, since radio receivers usually operate at low sampling rates, we resample in MATLAB the transient EMI waveform before performing the FFTs to simulate the processing of the receiver. The undersampling effect is more visible in the case of the LoRaWAN receiver since the sampling frequency is very low ($125\,\mathrm{kS\,s^{-1}}$). Figure 11 reveals the presence of certain frequency components in the transient EMI sequence seen by a LoRaWAN receiver which is the result of the aliasing phenomenon. For instance, the transient EMI regular sequence illustrated in this figure (blue curve) has an interval between transients equal to $5\,\mu\mathrm{s}$. So, if the sampling frequency was sufficiently high, we would see the frequency components $0\,\mathrm{Hz}$, $200\,\mathrm{kHz}$, $400\,\mathrm{kHz}$,..., which are the multiples of $1/5\,\mu\mathrm{s}$. However, we see in this figure the presence of the additional frequencies $25\,\mathrm{kHz}$ and $50\,\mathrm{kHz}$.

The undersampling phenomenon described above can also be analyzed in the time domain. To better explain that, let us consider a transient EMI sequence with a $5\,\mu\mathrm{s}$ regular interval between transients and a LoRaWAN receiver with a sampling frequency of $125\,\mathrm{kS\,s^{-1}}$ and therefore with a sampling period of $8\,\mu\mathrm{s}$. Knowing that each transient pulse only lasts a few ns, they will not always be detected. In fact, the detection depends on the time lag between the transient EMI signal at the input of the LoRaWAN receiver and the sampling sequence associated with the analog-to-digital converter (A/D). Consequently, the digitalized version of the transient EMI sequence and therefore its spectrum can be different each time an interference arrives at the radio receiver. A complete analysis of such a phenomenon requires a statistical approach. However, this is out of the scope of this paper and it can be explored in future works.

As a last remark, we highlight a qualitative difference between the red curves in Figs. 11 and Fig. 12. If, on one hand, the red curve in Fig. 11 preserves a regularity, on the other hand, no pattern is observed in the red curve in Fig. 12. This can be explained based on the transient EMI sequence length compared to the FFT size (which is equivalent to a LoRaWAN or LTE symbol time). In our tests, we create a transient EMI sequence with a duration of $500\,\mu\mathrm{s}$, which is constantly repeated over time (the referred duration is due to the signal generator memory constraint). During the symbol extraction process, a LoRaWAN receiver performs an FFT with $32.8\,\mathrm{ms}$ duration. During this period, the transient EMI sequence is repeated approximately 66 times. This periodicity in time creates a regular pattern in the frequency domain. On the other hand, the FFT performed by an LTE radio receiver has a duration of $66.7\,\mu\mathrm{s}$, which is inferior to the duration of the transient EMI sequence, so this effect is not observed.

VII. Conclusions

In this paper, we propose a test methodology to evaluate the immunity of wireless communication systems in the presence of transient radiated EMI. Our proposal fills a gap observed in the EMC literature, as the classical immunity test standards are usually dedicated to the validation of electronic products and not to the evaluation of communication solutions. Such a proposal is particularly important in the railway sector, where new wireless communication systems have recently been installed and still need to withstand the effects of transient sparks generated by the pantograph-catenary contact.

Among the many aspects of our methodology, we highlight the design of the EMI waveform and the definition of a harmonized resilience metric. The proposed EMI waveform addresses many objectives. First, it must faithfully represent real transients. This is based on a previous experimental study which shows that, unlike the regular transient sequences suggested by traditional immunity test standards, the repetition intervals of the transient EMI generated by the pantograph-catenary contact are highly variable. Second, the EMI waveform must have the same effect on the radio receiver regardless of the LoRaWAN/LTE communication channel selected for testing. The proposed waveform fulfills this objective if the chosen parameters ($\mathrm{RT} = 1\,\mathrm{ns}$, $\mathrm{TD} = 10\,\mathrm{ns}$) result in an approximately flat spectrum.

Concerning the resilience metric, we highlight that although we use specific error indicators for each communication system (timeout for LoRaWAN and BLER for LTE), the results are expressed in terms of a more general indicator: the critical SIR. Such an approach makes it easier to compare different communication systems in terms of EM immunity.

Experimental results suggest that the critical SIR of LoRaWAN and LTE systems can change depending on the regularity of the transients. In particular, LoRaWAN was shown to be more sensitive to these parameter changes than LTE. These results suggest that the way the test methodology is designed and the test parameters adopted can play a significant role in the results. Therefore, the results of an immunity test may be biased and provide unrealistic behavior if the test methodology is not well designed.

In addition, we have observed significant variability between successive repeated test results with transient interference, especially for LoRaWAN. Due to this variability, it may be relevant to consider the susceptibility analysis statistically, especially if the application does not permanently require maximum communication performance.

The aim of this work was to identify the parameters that can be harmonized or that need to be adapted to the communication system being tested. This contribution could allow the development of an EMC test standard dedicated to the evaluation and comparison of different wireless solutions for the railway industry. Such a standard can potentially be included in the homologation steps of trains.

Acknowledgment

We would like to thank Dr. Paul Monferran for his valuable help to improve the clarity of ideas of the manuscript.

References

[1] V. Deniau, T. Vantrovs, N. Becuwe, C. Gransart, A. N. De Sao Jose, A. Boe, E. P. Simon, O. Vlamynck, F. Valenti, J. Villain, and Q. Rivette,

"Analysis of the susceptibility of the lora communication protocol in the railway electromagnetic environment," in *2021 XXXIVth General Assembly and Scientific Symposium of the International Union of Radio Science (URSI GASS)*, 2021, pp. 1–4.

[2] A. Berti, "How is augmented reality changing rail operations?" Jan 2020. [Online]. Available: https://www.railway-technology.com/features/use-of-ar-in-rail/

[3] R. He, B. Ai, G. Wang, K. Guan, Z. Zhong, A. F. Molisch, C. Briso-Rodriguez, and C. P. Oestges, "High-speed railway communications: From gsm-r to lte-r," *IEEE Vehicular Technology Magazine*, vol. 11, no. 3, pp. 49–58, 2016.

[4] B. Ai, A. F. Molisch, M. Rupp, and Z.-D. Zhong, "5g key technologies for smart railways," *Proceedings of the IEEE*, vol. 108, no. 6, pp. 856–893, 2020.

[5] Y. Alsaba, M. Berbineau, I. Dayoub, E. Masson, G. M. Adell, and E. Robert, "5g for remote driving of trains," in *Communication Technologies for Vehicles*, F. Krief, H. Aniss, L. Mendiboure, S. Chaumette, and M. Berbineau, Eds. Cham: Springer International Publishing, 2020, pp. 137–147.

[6] S. Dudoyer, V. Deniau, R. Adriano, M. N. B. Slimen, J. Rioult, B. Meyniel, and M. Berbineau, "Study of the susceptibility of the gsm-r communications face to the electromagnetic interferences of the rail environment," *IEEE Transactions on Electromagnetic Compatibility*, vol. 54, no. 3, pp. 667–676, 2012.

[7] "Enabling and managing end-to-end resilience," https://www.enisa.europa.eu/publications/end-to-end-resilience/at_download/fullReport, accessed: 2023-07-24.

[8] N. Davari, B. Veloso, G. d. A. Costa, P. M. Pereira, R. P. Ribeiro, and J. Gama, "A survey on data-driven predictive maintenance for the railway industry," *Sensors*, vol. 21, no. 17, 2021.

[9] "Exploitation ferroviaire : Bientot une communication en 5g, howpublished = https://www.sncf.com/fr/groupe/newsroom/communication-ferroviaire-5g, note = Accessed: 2023-03-20."

[10] A. Mariscotti, "Critical review of emc standards for the measurement of radiated electromagnetic emissions from transit line and rolling stock," *Energies*, vol. 14, no. 3, 2021.

[11] X. Geng, Y. Wen, and J. Zhang, "An apd-based evaluation on the effect of transient disturbance over digital transmission," *Chinese Journal of Electronics*, vol. 29, no. 1, pp. 57–65, 2020.

[12] G. Boschetti, A. Mariscotti, and V. Deniau, "Assessment of the gsm-r susceptibility to repetitive transient disturbance," *Measurement*, vol. 45, no. 9, pp. 2226–2236, 2012.

[13] X. Geng, Y. Wen, J. Zhang, and D. Zhang, "A method to supervise the effect on railway radio transmission of pulsed disturbances based on joint statistical characteristics," *Applied Sciences*, vol. 10, no. 14, 2020.

[14] G. Gao, X. Yan, Z. Yang, W. Wei, Y. Hu, and G. Wu, "Pantograph–catenary arcing detection based on electromagnetic radiation," *IEEE Transactions on Electromagnetic Compatibility*, vol. 61, no. 4, pp. 983–989, 2019.

[15] M. Pous, M. A. Azpúrua, and F. Silva, "Measurement and evaluation techniques to estimate the degradation produced by the radiated transients interference to the gsm system," *IEEE Transactions on Electromagnetic Compatibility*, vol. 57, no. 6, pp. 1382–1390, 2015.

[16] Y. Lin, J. Zhang, Z. Tan, and X. Jin, "Analysis on radio immunity of td-lte to interference in high speed railway," in *2014 International Conference on Electromagnetics in Advanced Applications (ICEAA)*, 2014, pp. 574–578.

[17] O. Stienne, V. Deniau, and E. P. Simon, "Assessment of transient emi impact on lte communications using evm papr," *IEEE Access*, vol. 8, pp. 227 304–227 312, 2020.

[18] Y. Wang, X. Zhang, G. Zhu, S. Lin, and W. Wang, "Evaluation of lte-r system performance with pantograph-catenary arc interference," in *2020 IEEE International Symposium on Antennas and Propagation and North American Radio Science Meeting*, 2020, pp. 1277–1278.

[19] J. Wang, G. Wang, D. Zhang, J. Zhang, and Y. Wen, "The influence of pantograph arcing radiation disturbance on lte-r," in *2019 International Conference on Electromagnetics in Advanced Applications (ICEAA)*, 2019, pp. 0583–0586.

[20] "NF EN 50121-3-2 - Applications ferroviaires - Compatibilité électromagnétique Partie 3-2 : Matériel roulant - Appareils ," IEEE Electromagnetic Compatibility Society, Standard, May 2017.

[21] O. B. A. S. N. Sornin, "Low power long range transmitter," U.S. Patent 9,252,834, 2 February 2016.

[22] "Lorawan architecture," https://www.thethingsnetwork.org/docs/lorawan/architecture/, accessed: 2022-07-19.

[23] "RP002-1.0.3 LoRaWAN Regional Parameters," LoRa Alliance, Standard, May 2021.

[24] "LTE; Evolved Universal Terrestrial Radio Access (E-UTRA); User Equipment (UE) conformance specification; Radio transmission and reception; Part 1: Conformance testing (3GPP TS 36.521-1 version 16.6.0 Release 16) ," ETSI, Standard, 2020.

[25] N. Ben Slimen, V. Deniau, S. Baranowski, J. Rioult, N. Dubalen, B. Demoulin, and C. Railcom, "On board measurements of the railway's electromagnetic noise with moving train," in *2007 18th International Zurich Symposium on Electromagnetic Compatibility*, 2007, pp. 365–368.

[26] M. Jin, M. Hu, H. Li, Y. Yang, W. Liu, Q. Fang, and S. Liu, "Experimental study on the transient disturbance characteristics and influence factors of pantograph–catenary discharge," *Energies*, vol. 15, no. 16, 2022.

[27] "Telecommunication network equipment; harmonised standard for electromagnetic compatibility (emc) requirements (draft etsi en 300 386 v2.2.0 2020-10)," ETSI, Standard, 2020.

[28] N. Artur, E. P. Simon, A. Boe, T. Vantroys, C. Gransart, and V. Deniau, "A methodology to estimate the signal-to-interference power ratio for intermittent disturbances," in *2021 XXXIVth General Assembly and Scientific Symposium of the International Union of Radio Science (URSI GASS)*. IEEE, 2021, pp. 1–4.